

Biospeckle laser for assessing tomatoes ripeness indexes¹

Fernanda Fernandes Adimari Pavarin^{2*}, Juliana Aparecida Fracarolli³, Alexandre Xavier Falcão⁴

ABSTRACT - The quality perception of fruits and vegetables is a key factor for marketing and consumption. Quality determination is carried out subjectively by the consumer and with objective methods, many of which are destructive. The use of optical techniques and real-time screening, including determination of quality attributes by non-destructive methods, represents operational advantages for grading and selection systems. This work aimed to search for correlation between the tomato ripeness indexes with Biospeckle Laser (BSL) data. The epidermis color (CIE L*a*b), firmness, pH, Total Titratable Acidity (TTA), Total Soluble Solids (TSS), (°Brix), and respiration were measured. These data were correlated with BSL numerically by the Moment of Inertia (MI) and the Average Value of Difference (AVD). A high correlation was found with respiration and pH by the MI method, and with TTA, flavor, and respiration by the AVD method.

Key words: Post-harvest. Image analysis. Tomato-ripening. BSL.

DOI: 10.5935/1806-6690.20240022

Editor-in-Chief: Eng. Agrônomo, Manoel Barbosa Filho - manael.filho@ufc.br

*Author for correspondence

Received for publication 30/10/2020; approved on 25/07/2023

¹This research was part of the master's thesis of Fernanda Fernandes Adimari Pavarin and was funded by the National Council for Scientific and Technological Development (CNPq)

²School of Agricultural Engineering (FEAGRI), University of Campinas (UNICAMP), Campinas-SP, Brazil, ffadimari@yahoo.com.br (ORCID ID 0000-0002-5235-8659)

³School of Agricultural Engineering, Postharvest Technology, University of Campinas (UNICAMP), Campinas-SP, Brazil, juliana.fracarolli@gmail.com (ORCID ID 0000-0001-8793-3185)

⁴Institute of Computing (IC), University of Campinas (UNICAMP), Campinas-SP, Brazil, alexandre.falcao@gmail.com (ORCID ID 0000-0002-2914-5380)

INTRODUCTION

In post-harvesting, the selection and classification stages directly influence the commercialization and play an important role in the economy, since they determine the value of what is being marketed, generating a significant economic impact for the buyer and seller (FERREIRA; QUADROS; FREITAS, 2005).

Climacteric fruits, such as tomatoes, are characterized by metabolic changes from the development phase to ripening, having as a peculiarity a marked and brief ripening phase followed by a peak of respiration, even after being harvested (COLOMBIÉ *et al.*, 2016).

Products with different degrees of ripeness and size should be separated. A selection by ripeness, size, shape, injuries, and defects must be carried out with discretion. The selection process is a traditionally manual craft in Brazil, but it is a market that seeks professionalization and new technologies to meet the quality demands of national and international markets.

The Biospeckle Laser (BSL) technique applied to agricultural products provides information related to cellular activities in a non-destructive manner. The cellular activity detected by BSL can be related to various processes such as cell growth, cell division, or any other process represented by the movement of cell organelles, biochemical reactions, or cytoplasmic movements. This cellular activity causes the movement of microscopic molecules and structures that create the interference pattern known as dynamic speckle, which can be used to measure changes in the biological functioning of cells and tissues, such as the physiological changes during the fruit ripening process (CARDOSO *et al.*, 2011).

The development of sensors for real-time sorting allows for the selection and classification process to be automatic, non-destructive, objective, and quick. Among the sensors used, those based on the visible spectrum, multispectral, hyperspectral, X-ray (MAHANTI *et al.*, 2022), terahertz, Raman spectroscopy (CAKMAK, 2019) stand out. However, some of these technologies involve high-cost sensors, in addition to high computational demands that hinder their commercial use (PALUMBO *et al.*, 2023). In this sense, biospeckle has advantages since it allows the evaluation of the surface of the products and even the internal layers of the plant tissue, since the speckle pattern is influenced by the biological processes within the cells (ZDUNEK *et al.*, 2014).

The laser, as a light source, penetrates the subsurface layers and, although the technique makes use of sensors in the visible spectrum, it can evaluate agricultural products with simple and low-cost equipment (PANDISELVAM *et al.*, 2020).

Thus, this work aims to evaluate the efficiency of an optical analysis technique, BSL, to determine quality attributes in tomatoes in a non-destructive way, helping classification and selection process.

MATERIAL AND METHODS

Tomatoes cv. Compack (DRW 7698), from Monsanto, from Sítio Candelária, located in Sumaré – SP, with approximate coordinates of 22°49'18" S and 47°16'00" W and altitude of 573 m above sea level, were used. This variety can be grown in summer and winter, allowing two harvests per year, with good resistance to diseases, fruits with a firm texture, called long life, with average values of caliber and mass of 78 mm and 220 grams, respectively.

Fruits harvested at Stage 1, green, were sanitized to remove impurities, immersed in a 2.5% sodium hypochlorite solution for 15 minutes, and dried. They were then stored at 12 °C.

A total of 20 tomatoes were used for each stage of ripening. After daily monitoring, tests were performed as the stages were reached, based on the change in color according to the USDA standard (UNITED STATES DEPARTMENT OF AGRICULTURE, 1991).

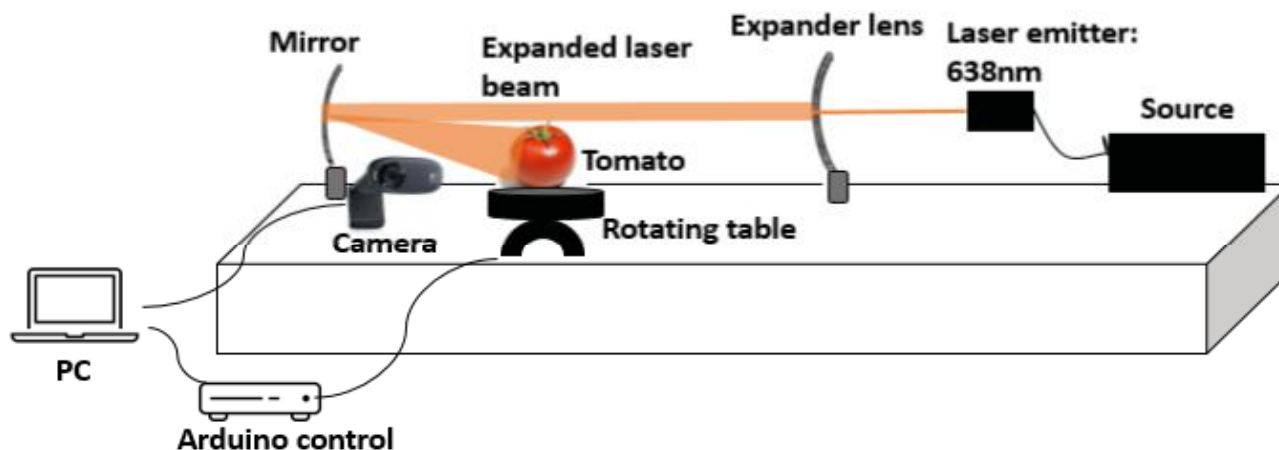
The study design was completely randomized. The treatment comprised six different ripening stages, with 10 replicates for each variable.

Step 1 – BSL Assays

The biospeckle assay was performed with the Laserline® iZi 638 diode laser module, with 638 nm wavelength and 5 mW of power. This model had a point emitter and active temperature stabilizer, which allows for greater power and wavelength stability.

To evenly bathe the entire fruit surface in laser light, the setup employed a mirror and a beam expander lens. The laser first passed through the lens, expanding its beam, then bounced off the mirror and into a light box with an infinity curve. The tomato was positioned in the center of the light box. A Logitech® C920 camera coupled to a personal computer with an Intel® Core i7 processor was used to capture the laser images. This configuration, shown in Figure 1, remained untouched throughout the experiment.

A 20-second film was recorded with no light in the environment except for the laser illuminating the tomato. A total of two films were recorded, one for every 180° fruit rotation. The camera autofocus has been disabled during capture to avoid external interference. Figure 2 shows the image of the laser acquisition.

Figure 1 - Experimental setup of the BSL assay

Source: Prepared by the author

Figure 2 - Image taken during laser filming

Source: Prepared by the author

Films were segmented into frames using the Free Video to JPG Converter from Free Studio®. A total of 228 frames were obtained to discard the first 100, resulting in 128 frames to process the BSL results.

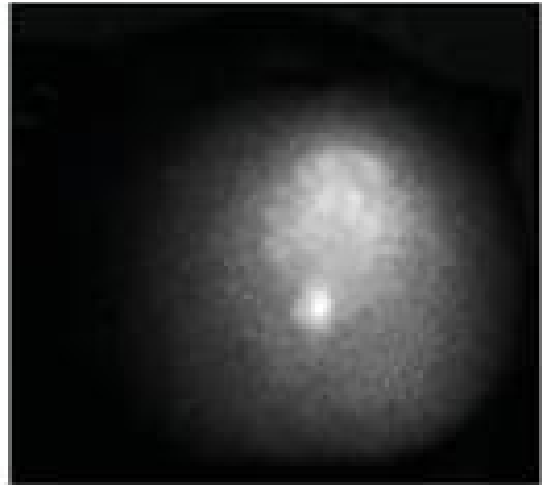
The originally color images were transformed to grayscale, a step performed using the ImageJ® program, by changing the image to 8-bit, as shown in Figure 3.

For the analysis of BSL events, the procedure developed by Braga, Rivera e Moreira (2016), with routines using the OCTAVE program, was used. This procedure works by loading the Biospeckle Laser Tool Library (BSLTL) software which allows obtaining the numerical results Moment of Inertia (MI) and Average Value of Difference (AVD), and the images referring to the Fujii and DG methods.

According to Rabal e Braga (2008), this dynamic speckle phenomenon and its properties have been studied theoretically and experimentally by vibrations and velocity and displacement measurements. Studies carried out on inanimate and rigid objects show the influence of dispersion on them, but in living materials the dynamic speckle has different characteristics, and multiple dispersions must be considered since the dynamics of a living cell is different from that of an inanimate material.

There are two types of speckle pattern, one translational and one boiling. In the translational, the speckle grain pattern remains motionless and when displacements occur in the object the speckle grain pattern moves as a whole. In the boiling pattern, on the other hand, the movements of the speckle grain is chaotic and similar to a boiling liquid, and the grain pattern moves, deforms, appears, and disappears without any change in the object's position. The latter is typical of living materials (RABAL; BRAGA, 2008).

Oulamara, Tribillon e Duvernoy (1989) propose one way to show the temporal evolution of a speckle pattern, consisting of recording successive images of the dynamic speckle pattern for each state of the evaluated phenomenon. A particular column is selected in each of the images. Then, a new image is constructed by placing the column extracted from the initial image side by side, successively. The resulting image is called a time history speckle pattern (THSP). Its rows represent different points in the grain pattern, and its columns its intensity in a sequence of regularly spaced time intervals. The activity of the sample appears as the intensity and changes in the horizontal direction, that is, along the lines (ARIZAGA; TRIVI; RABAL, 1999).

Figure 3 - Converting Laser Images to grayscale

Source: Prepared by the author

The Moment of Inertia of the Co-Occurrence matrix is used as a measure of biospeckle activity in some applications, according to Rabelo *et al.* (2011). To obtain a quantitative measurement of M_{CO} , it is necessary to normalize it first. This is done by dividing each row of the matrix by the number of times the first level of gray appeared and is given by Equation (1).

$$M_{ij} = \frac{N_{ij}}{\sum_j N_{ij}} \quad (1)$$

A measure of the spread of the M-values around the principal diagonal can be constructed as the sum of the matrix values by multiplying their square distance of rows to the principal diagonal. This is a particular second-order moment, also called the moment of inertia of the matrix with respect to this diagonal in the direction of the line, and is given by Equation (2).

$$MI = \sum_{ij} M_{ij} (i - j)^2 \quad (2)$$

This calculation is done in such a way that low pixel intensity variations will add low values to the final MI value, whereas high variations will contribute more to the MI value. For example, when considering the change in intensity of a pixel from 0 to 255, $(0 - 255)^2 = (-255)^2 = 65,025$ will be added to the final MI value. However, if the change is from 60 (value of i) to 40 (value of j), $(60 - 40)^2 = 400$ is added to the final MI value. In this way, if the phenomenon shows small changes in the speckle patterns, the MI will add less value to quantify it (ANSARI; NIRALA, 2013).

According to Braga *et al.* (2011) and Zdunek *et al.* (2014), the Average Value of Difference (AVD) numerical method emerges as an alternative to the routine MI method. It is based on the principle that the sum of the

differences is the main information researched and that the square operation performed in the MI method can amplify the variations in the time history in a distorted way. Thus, the AVD calculation does not take a square operation according to Equation (3).

$$AVD = \sum_{ij} \{M_{ij} |i - j|\} \quad (3)$$

Stage 2: Determination of ripening parameters

CIE L*a*b* Color Determination

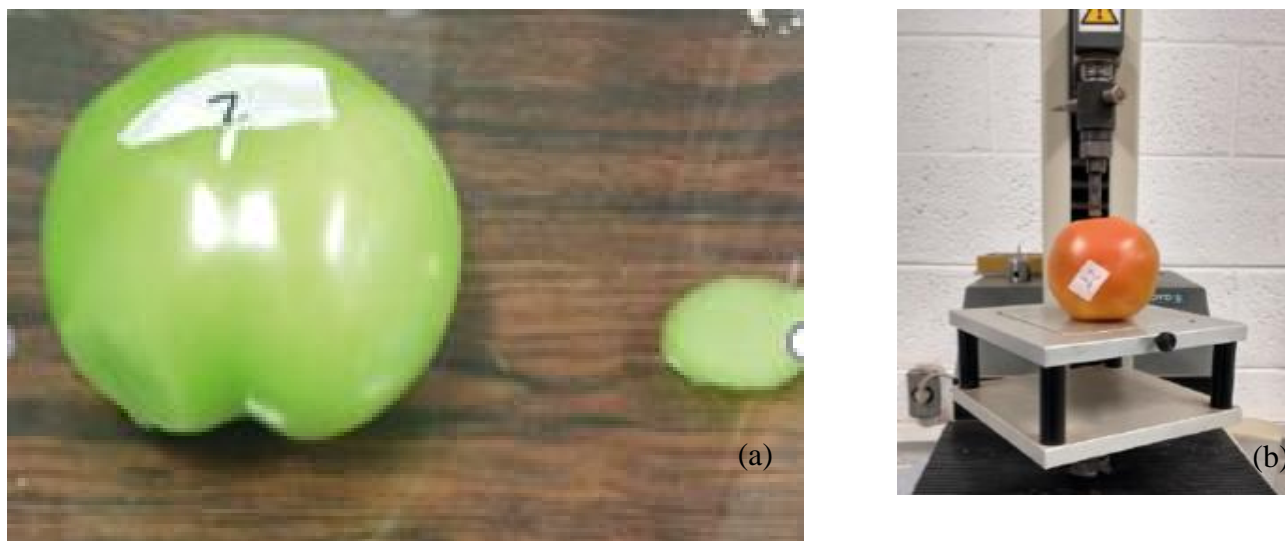
For the color attributes, a Konica Minolta® spectrophotometer model CM-700d was used, which quantifies spectral data through the light reflected by the objects at each wavelength to determine the color coordinates of the object in the color space L*a*b* and presents the information in numerical terms.

The equipment was calibrated to the white standard at the beginning of the tests for each stage. After calibration, three color readings were performed for each tomato and an average was obtained to calculate the a*/b* ratio.

Firmness Tests

The firmness tests was carried out with the Texture Analyser TA500 universal testing machine from Lloyd Instruments with a 0.5% accuracy. The measurements were performed after the removal of the tomato epidermis, in an area of approximately 1cm², on two diametrically opposite faces, as shown in Figure 4. Subsequently, a mean of these values was considered in the analyses.

The 7.9 mm diameter flat-face penetration tip was positioned over the skinless area, descending at a constant rate of 1 mm/s and with a maximum course of 10 mm penetration. The maximum stress was obtained by a load

Figure 4 - Details of sample preparation and equipment used in the firmness test

(a) Removal of part of the tomato epidermis for the test (b) Detail of the positioning of the sample in the load cell and the penetration tip. Source: Prepared by the author

cell of 50 kilogram-force (kgf), recorded in Newtons (N) using the Nexygen® program.

Total Soluble Solids (TSS)

An ATAGO portable refractometer, model ATC-1 (Automatic Temperature Compensation), 0.1% scale and measurement accuracy ± 0.2 Brix, was used to measure TSS.

Before measuring the sample, the refractometer was calibrated with distilled water at room temperature.

The sample was crushed and homogenized for three minutes with a hand mixer. Some drops of the homogenized material were placed on the surface of the prism, generating the direct measurement.

Total Titratable Acidity (TTA) and pH

The pH of the homogenized material was recorded before the beginning of the titrations. Then, 10 g of the homogenized material was weighed in 150 mL beakers, to which 90 mL of distilled water were added.

Each sample was titrated with the addition of a NaOH solution (0.1 N) until 8.1 pH was reached, with constant agitation, at which point it is considered that all citric acid, the predominant organic acid in tomatoes, was titrated. The acidity of the solution can be expressed as a percentage according to Equation 4 (INSTITUTO ADOLFO LUTZ, 2008).

$$TTA = \frac{V \cdot F \cdot M \cdot MW}{10 \cdot W \cdot n} \quad (4)$$

Where V is the volume of the sodium hydroxide solution used in the titration; F is the correction factor of

the sodium hydroxide solution; M is the molarity of the sodium hydroxide solution; MW is the molecular weight of the corresponding acid in g; W is the mass of the sample in g; and n is the number of ionizable hydrogens.

Respiration

Respiratory rate measurement was performed with a gas composition analyzer (CO₂ and O₂) Pac Check 325 MOCON®. A total of 10 samples from each stage were separated and individually packed in glass containers with lids with holes sealed with silicone, to allow only the passage of the equipment reading tip, preventing gas exchange with the environment.

The whole fruits were packed in containers and kept at 10 °C for 1 hour, with %CO₂ readings every 0.5 h.

The calculation of the CO₂ production rate is given by Equation (5):

$$CO_2 = \frac{\%CO_2}{100} \cdot \frac{V_{empty}}{m_{product}} \cdot \frac{1.98}{t} \quad (5)$$

Where %CO₂ is the reading obtained by the equipment, V_{empty} is the total volume of the glass container minus the volume of the product, m_{product} is the mass of the product, t is the time in hour of pre-reading storage, 1.98 is the conversion of mL of CO₂ to mg of CO₂. The result is expressed as mg CO₂/kg h (BARBOSA, 2013; BETIN *et al.*, 2018).

The results were evaluated by analysis of variance (ANOVA) using Tukey's test with 5% significance. All statistical analyses were performed using the Sisvar® statistical program (FERREIRA, 2011).

RESULTS AND DISCUSSION

The tomato ripening stages were characterized by physicochemical analyses, starting with classification according to color. This criterion is the visual differential between the ripening stages. For the CIE L*a*b* color attribute analyses, the values shown in Graph 1 were obtained according to Tukey's test at 5% significance.

These results are similar to the values found in the literature by Arias *et al.* (2000) and Camelo and Gómez (2004), allowing us to affirm that this relationship follows the trend of growth in the a*/b* ratio values as the ripening stages evolve.

By ANOVA, all stages could be differentiated, excepting Stages 3 and 4, which did not differentiate between the means, as shown in Table 1. The minimum value found was for Stage 1, a*/b* = -0.25, and the maximum was for Stage 6, a*/b* = 0.86. The results indicate that statistically identifying the different ripening stages is possible at a 5% significance level.

The firmness test yielded results similar to those reported in the literature, with a tendency for higher firmness in the greener stages and less firmness for the ripe stages, as shown in Graph 2 (LIEN; AY; TING, 2009).

Means for Stages 2, 3 and 4 did not differ. Since these are intermediate stages, the results of some quality attributes can be difficult to differentiate due to the proximity of the stages. Stages 1, 100% unripe, and 5 and 6, riper, presented results that differentiated them, with values of 33.51 ± 2.65 N, 10.10 ± 0.65 N, and 8.12 ± 0.70 N for Stages 1, 5 and 6, respectively.

The texture of the tomatoes can be classified, according to Kader (2002), from very firm to very soft, evolving gradually between the ripening stages, as shown in Graph 2.

Genetic and management traits, such as tillage and fertilization, have a great influence on quality attributes. Tomato cv. Compact is classified as long-life, so it remains firmer as the ripening stages evolve.

Graph 1 - Color attribute results – a*/b* ratio of CIE L*a*b space

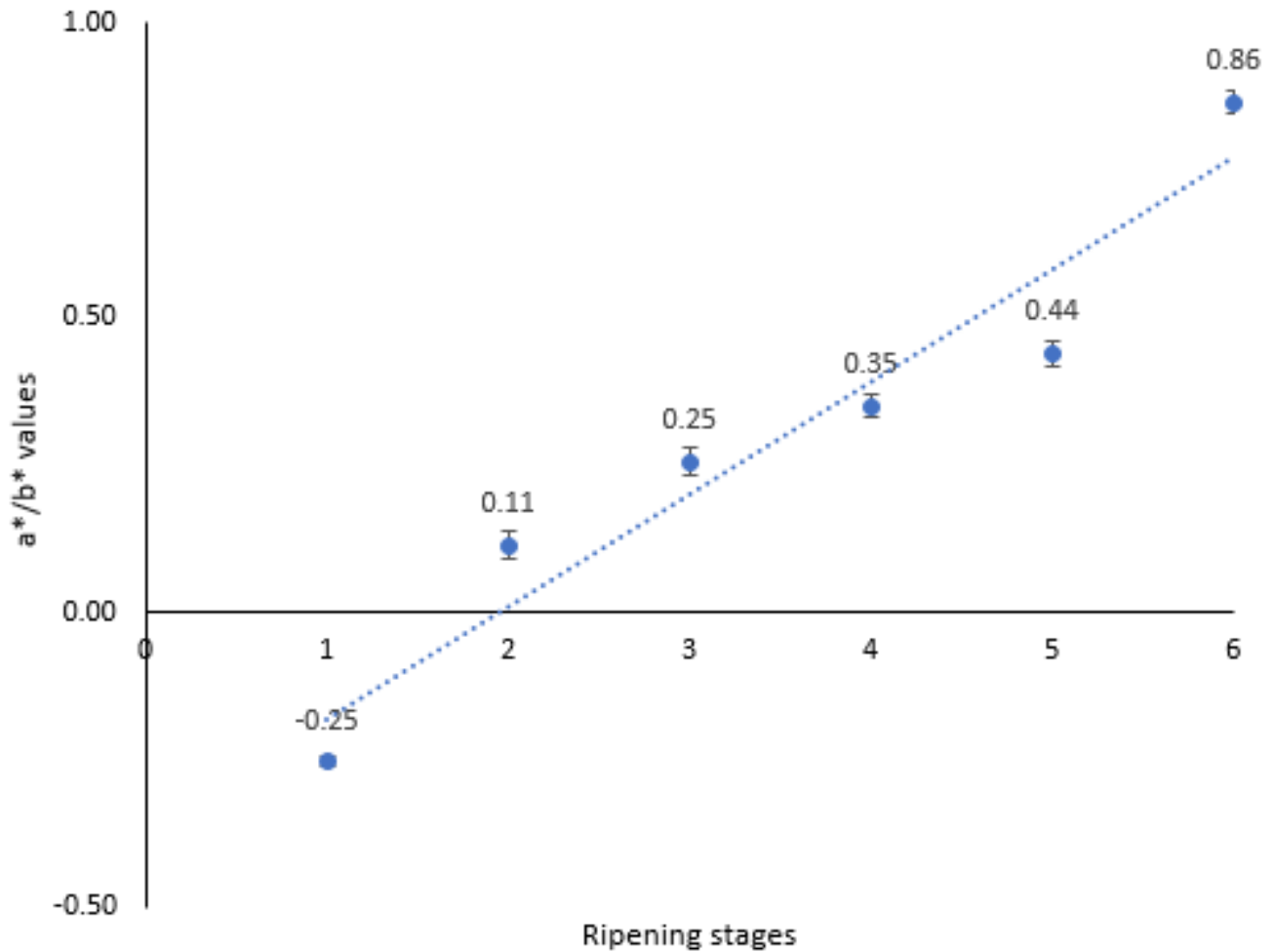
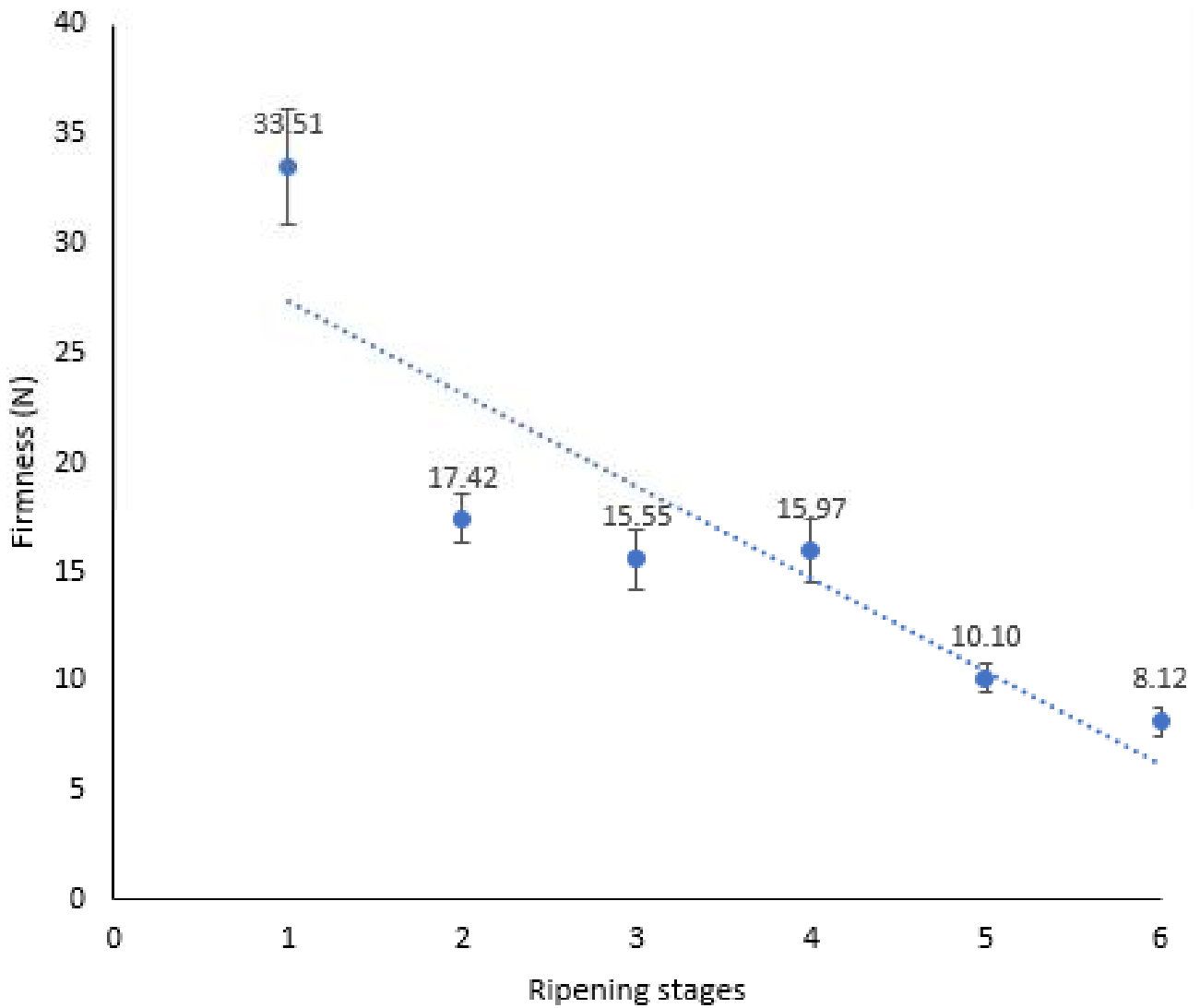


Table 1 - Analysis of variance means and summary for a*/b* ratio

Ripening stage		a*/b*			
1	-0.254	(a)			
2	0.097	(b)			
3	0.257	€			
4	0.312	(c)			
5	0.426	(d)			
6	0.842	(e)			
FV	GL	SQ	QM	p-value	
Stages	5	6.574	1.315	0.0000	
Error	54	0.380	0.007		
Total	59	6.953			
CV	29.95%				

Graph 2 - Firmness results (N)



According to Moura *et al.* (2005), the higher firmness of mutant fruits, such as the Compack variety, may be related to the delay in the increase in polygalacturonase activity, therefore, leading to firmer mutant fruits than normal ones even when fully ripe.

The results of TTA, pH and TSS were obtained after crushing and homogenizing the samples. Table 2 shows the results.

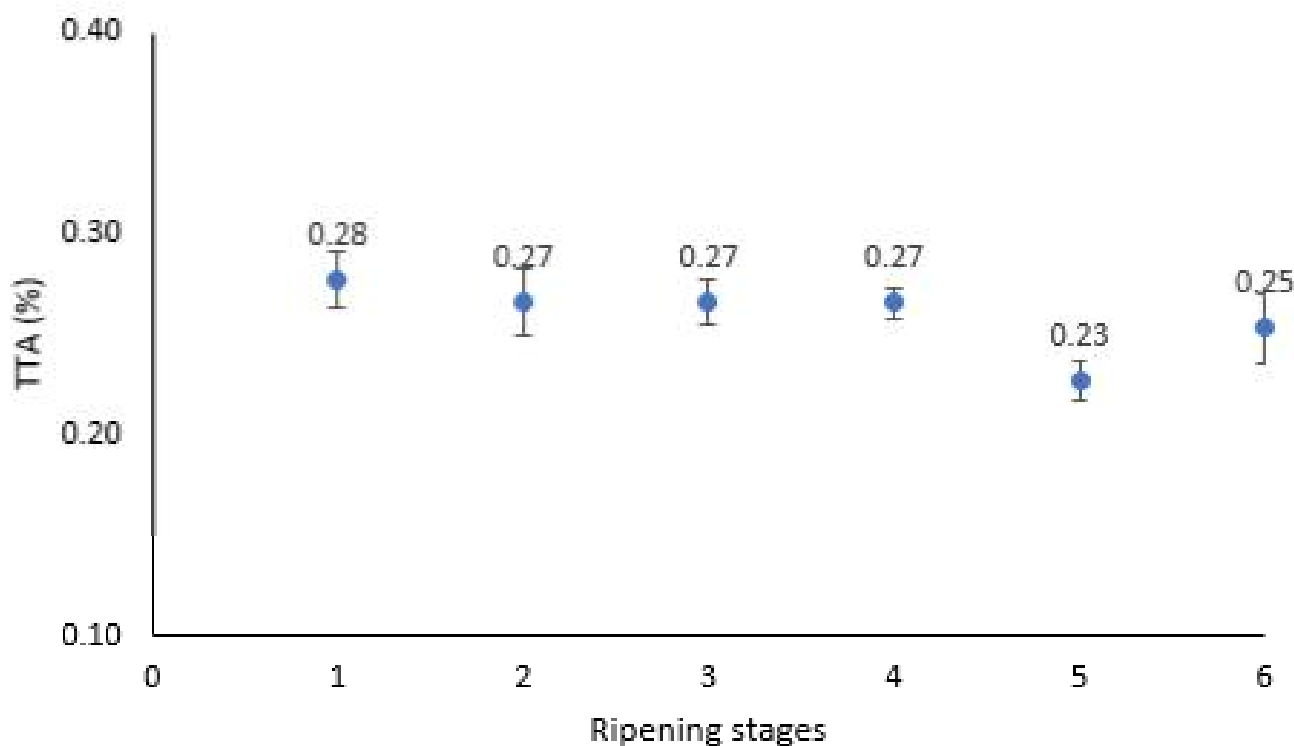
The TTA results did not show any differentiation between the means, as shown in Table 2, where p-value > 0.05 for a 5% significance. The total acidity in fruits expresses the amount of organic acids that may be related to tomato astringency.

Similar variations were found in the literature with values between 0.23% and 0.28%, based on citric acid (FERREIRA *et al.*, 2010; SHIRAHIGE, 2010). Graph 3 shows the result of the means.

Table 2 – Analysis of variance means and summary of for TTA, pH, and TSS

Ripening stage	TTA %				pH				TSS oBrix			
1	0.276	(a)			5.30	(c)			4.11	(a)		
2	0.268	(a)			5.49	(d)			4.03	(a)		
3	0.268	(a)			5.49	(d)			4.04	(a)		
4	0.264	(a)			5.00	(b)			4.12	(a)		
5	0.228	(a)			5.88	(e)			4.03	(a)		
6	0.267	(a)			4.59	(a)			4.04	(a)		
FV	GL	SQ	QM	p-value	GL	SQ	QM	p-value	GL	SQ	QM	p-value
Stages	5	0.015	0.003	0.1533	5	9.971	1.994	0.0000	5	0.868	0.017	0.9361
Error	54	0.093	0.002		54	1.087	0.020		54	3.695	0.068	
Total	59	0.107			59	11.058			59	3.782		
CV	15.85%				2.68%				6.44%			

Graph 3 - Means obtained for Titratable Total Acidity (based on citric acid)



Among the organic substances in tomatoes, sugars, as measured by TSS, and organic acids are the most important constituents for the taste of the fruit. Sugars tend to increase progressively with the ripening of the fruit, whereas acidity increases at the initial ripening stage and then tends to decline. For this variety, this behavior was not observed, and the total acidity remained constant in all stages.

For the pH the mean values differed by stage, as shown in Table 2.

The values obtained for pH ranged from 4.59 ± 0.05 to 5.88 ± 0.02 . Mubarok *et al.* (2019) working with tomatoes of the varieties 'Mutiará,' 'Intan,' and 'Ratna' found pH values close to 4 and observed that the values decreased during the period of analysis for the variety 'Mutiará.' Al-Shaibani and Greig (1979) report that pH decreases significantly with the first signs of ripening and increases slightly from the ripe stage onwards (5 and 6). The tomato, during the process known as decomposition or senescence, starts to present changes in the concentration of hydrogen ions and consequently its pH and acidity change. Graph 4 shows an increase in pH at ripening Stage 5.

Shirahige (2010) found pH values of 4.07 to 4.23 and Al-Shaibani and Greig (1979) found pH values of 4.30 to 4.53 for ripe fruits of the Jetstar variety and pH of 4.14 to 4.52 for fruits of the Floramerica variety.

The TSS results did not differ between means, according to the ANOVA summary in Table 2, with p-value = 0.9361.

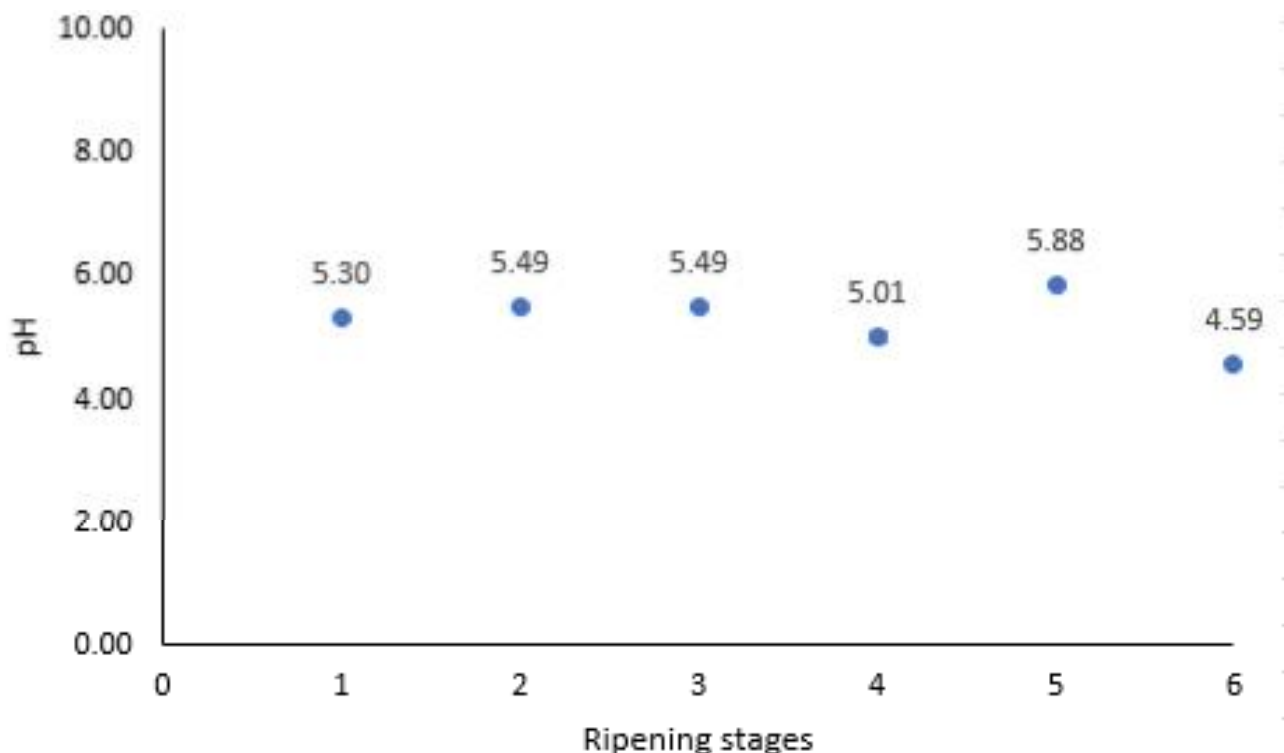
The values found are in line with the literature (FERREIRA *et al.*, 2010; SCHWARZ *et al.*, 2013). Sugars represent an important factor in the quality of tomatoes, corresponding to approximately 55% to 65% of the soluble solids fraction, also contributing to the overall aroma and flavor of the fruit. Tomatoes accumulate reducing sugars throughout fruit ripening, with little or no accumulation of sucrose. In ripe fruit, these sugars, such as fructose and glucose, together with organic acids constitute the typical sweet/sour taste of the fruits. Graph 5 shows the behavior of TSS by stage.

The flavor results, obtained by the TSS/TTA ratio, observed in Graph 6, presented values compatible with those of the literature, with values between 14.51 and 17.72 found by Shirahige (2010).

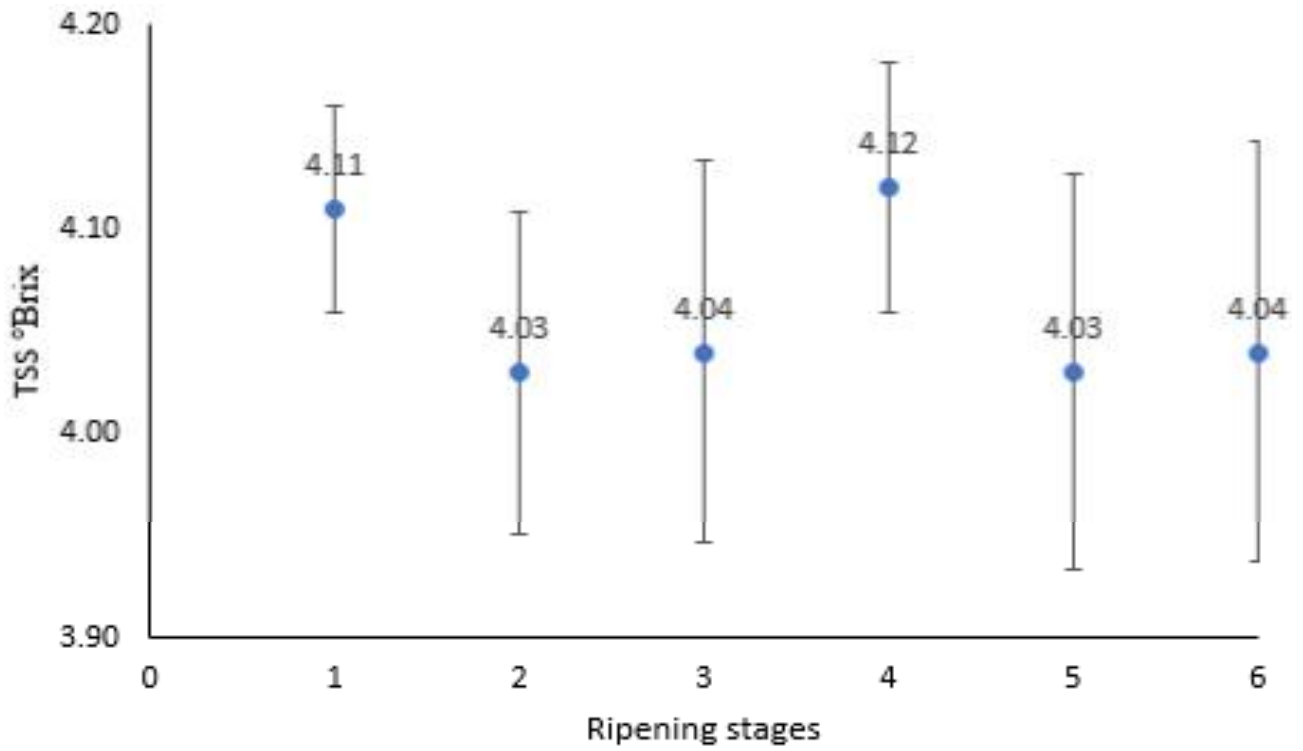
Since flavor is the ratio between sugars and acids, and based on results previously obtained for TSS and TTA, we observed a peak in flavor at stage 5, characterizing the stage as the one in which the flavor and aroma of the fruit would be more apparent.

Table 3 shows the values obtained in the ANOVA for flavor, showing that the difference between the means per ripening stage does not occur for TSS, with a p-value above 0.05.

Graph 4 - Means obtained for pH



Graph 5 - TSS Means



Graph 6 - Means for flavor

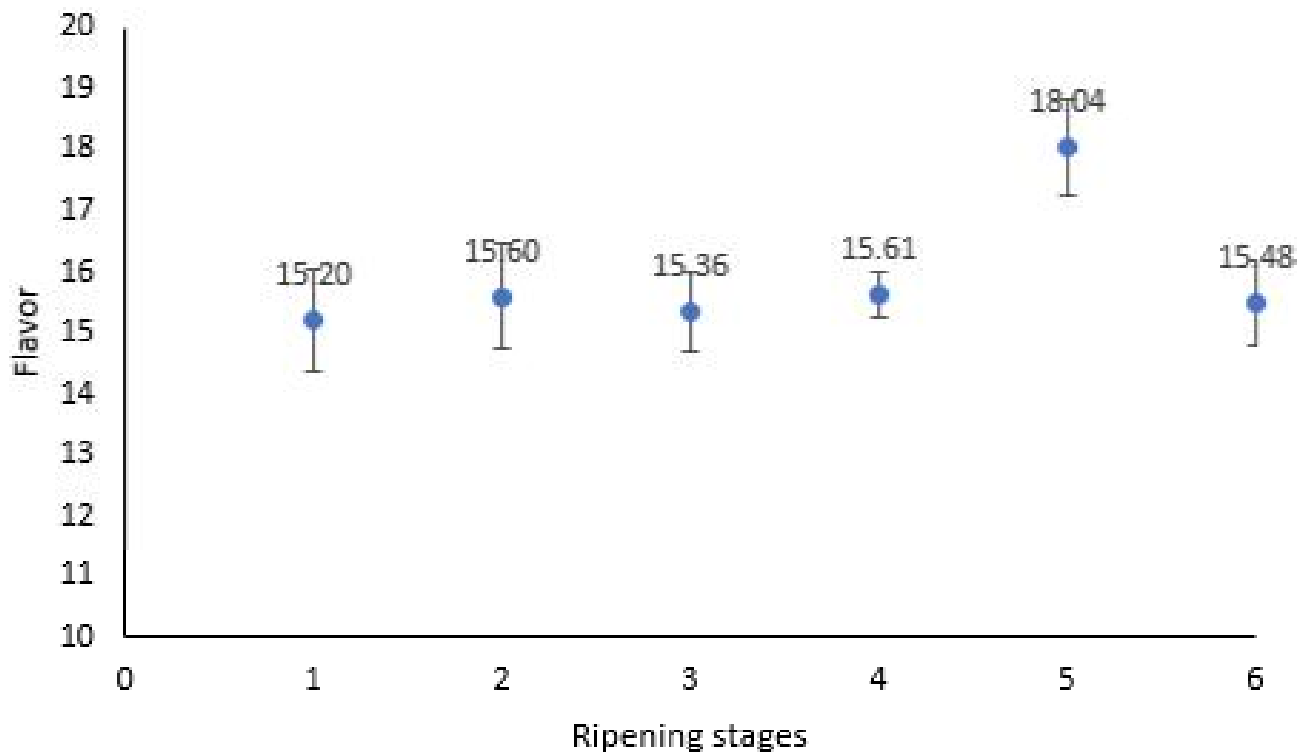


Table 3 - Analysis of variance means and summary for flavor

Ripening stage		Flavor			
1	15.2(c)				
2	15.59(d)				
3	15.37(d)				
4	15.61(b)				
5	18.04(e)				
6	15.48(a)				
FV	GL	SQ	QM	p-value	
Stages	5	57.047	11.409	0.0664	
Error	54	278.659	5.161		
Total	59	335.706			
CV	14.30%				

Table 4 - Analysis of variance mean and summary for respiration

Ripening stage	Respiration 0.5 h (mg CO ₂ /kg h)				Respiration 1 h (mg CO ₂ /kg h)			
	GL	SQ	QM	p-value	GL	SQ	QM	p-value
1	96.35	(c)			57.53	(a)		
2	67.77	(a)			56.07	(a)		
3	75.27	(ab)			50.93	(a)		
4	100.20	(c)			55.93	(a)		
5	92.45	(bc)			48.69	(a)		
6	85.38	(abc)			45.59	(a)		
FV	GL	SQ	QM	p-value	GL	SQ	QM	p-value
Stages	5	7978.86	1595.37	0.0001	5	1142.31	228.06	0.0566
Error	54	13292.44	246.49		54	5343.36	98.945	
Total	59	21270.230			59	6485.567		
CV	18.19%				18.96%			

Respiration is one of the most important biological activities in post-harvest, especially for climacteric fruits such as tomatoes. Table 4 shows the results for respiration after 0.5 h and 1 h.

The means in the different stages after 1 hour of storage did not differ, only those at 0.5 h, as shown in Graph 7.

The behavior of increasing the rate in the period prior to ripening was observed for stage 4, decreasing during ripening until senescence, as found in the literature (CHITARRA; CHITARRA, 2005; KADER, 2002; MOURA, 2002).

The increase in climacteric respiration depends on temperature and under optimal conditions can represent a 2 to 4 fold increase depending on the fruit, and compared with pre-climacteric respiration rates. At reduced temperatures, some fruits, such as tomatoes,

simply cease to show the climacteric peak, in this case at 8 °C (CALBO; MORETTI; HENZ, 2007).

Table 5 shows the means of the numerical results of the BSL assay. A differentiation could be found between the means for the two numerical methods applied, MI and AVD, as well as by the p-value lower than 0.05.

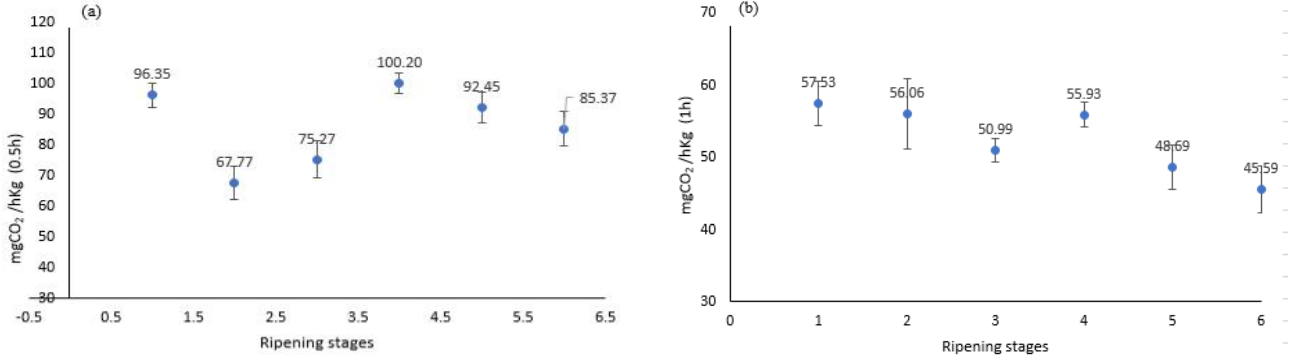
The results showed non-linear behaviors, Graph 8, starting with higher values followed by a drop and then showing a peak in the last stages. This behavior was observed in both the MI and AVD methods.

The physicochemical results were paired with the BSL results and for the MI a high correlation with respiration (0.5 h) was obtained, with a value of $R^2 = 0.7849$ for the second-order polynomial equation $y = -0.3155x^2 + 8.9342x + 33.124$. Another moderate correlation was obtained for pH, with $R^2 = 0.617$ for the third-order polynomial equation $y = -0.0023x^3 + 0.0771x^2 - 0.7956x + 7.8735$.

The AVD method also showed a high correlation with TTA, obtaining $R^2 = 0.8588$ for the equation $y = 0.3382x^3 - 1.765x^2 + 2.9621x - 1.3404$ and with flavor, resulting in $R^2 = 0.8038$ and third order polynomial fit equation $y = -17.659x^3$

$+ 90.971x^2 - 150.35x + 95.726$. Another moderate correlation was found with respiration (1 h) ($R^2 = 0.6382 / y = 100.16x^3 - 544.23x^2 + 955.78x - 489.08$). The other parameters showed low correlation with AVD data.

Graph 7 - Analysis of variance mean for CO₂ rates per ripening stage

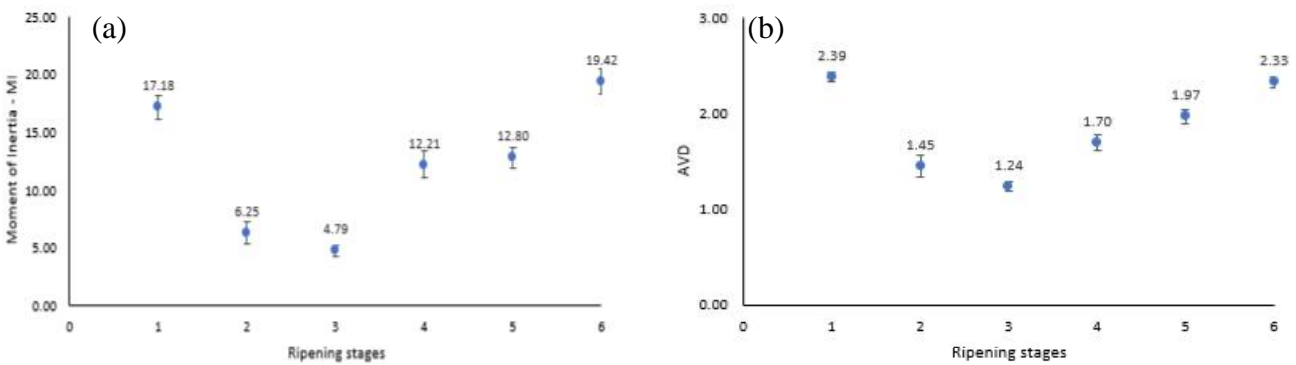


(a) CO₂ rates for 0.5 h time (b) CO₂ rates for 1 h time

Table 5 - Analysis of variance means and summary for MI and AVD

Ripening stage		MI			AVD			
1	17.18	(bc)			2.39	(c)		
2	6.25	(a)			1.45	(a)		
3	4.79	(a)			1.24	(a)		
4	12.21	(b)			1.70	(ab)		
5	12.8	(b)			1.97	(bc)		
6	19.426	(c)			2.33	(c)		
FV	GL	SQ	QM	p-value	GL	SQ	QM	p-value
Stages	5	1675.892	335.178	0.0000	5	10.845	2.169	0.0000
Error	54	937.248	17.356		54	6.497	0.120	
Total	59	2613.140			59	17.343		
CV	34.41%				18.79%			

Graph 8 - Analysis of variance means for numerical BSL results



(a) Moment of inertia (b) AVD method

The correlations obtained confirm the technique sensitivity for the visualization of biological phenomena such as respiration, according to ALVES *et al.* (2013). Other studies have also measured the correlation with other ripening parameters, such as Szymanska-Chargot, Adamiak, and Zdunek (2012) who found a strong correlation with firmness and Rabelo, Braga Júnior and Fabbro (2005) who studied the technique to monitor orange ripening.

We took care to mitigate noise and vibrations in the BSL image capture environment. Sound interference can affect speckle patterns increasing experimental error.

CONCLUSIONS

1. Differentiating ripening stages is possible by using the two biospeckle methods: MI and AVD;
2. The MI method found a high correlation with the respiration attribute and pH, and a weak correlation with TTA, color, firmness, flavor, and TSS;
3. Using AVD, a high correlation was found with flavor and TTA, moderate correlation with respiration, and low correlation with color, firmness, pH, and TSS;
4. For both methods, respiration was the parameter that allowed a moderate to high correlation with BSL;
5. Biospeckle is a promising method for identifying ripening stages in tomatoes. Future studies aimed at avoiding ambient noise would be important to develop this methodology on a production scale.

ACKNOWLEDGMENTS

This study was carried out with support from CNPq. I am grateful for the scholarship awarded for the 133031/2018 process, and for the funding of the project entitled Three-Dimensional Reconstruction of Fruits with Biospeckle, for the 424016/2016-8 process.

REFERENCES

AL-SHAIBANI, A. M. H.; GREIG, J. K. Effects of ripening stage, storage and cultivar on some quality attributes of tomatoes. **Journal of the American Society of Horticultural Science**, v. 104, n. 6, p. 880-882, 1979.

ALVES, J. A. *et al.* Identification of respiration rate and water activity change in fresh-cut carrots using biospeckle laser and frequency approach. **Postharvest Biology and Technology**, v. 86, p. 381-386, 2013.

ANSARI, M. Z.; NIRALA, A. K. Assessment of bio-activity using the methods of inertia moment and absolute value of the differences. **Optik**, v. 124, n. 6, p. 512-516, 2013.

ARIAS, R. *et al.* Correlation of lycopene measured by HPLC with the L*, a*, b* color readings of a hydroponic tomato and the relationship of maturity with color and lycopene content. **Journal of Agricultural and Food Chemistry**, v. 48, n. 5, p. 1697-1702, 2000.

ARIZAGA, R.; TRIVI, M.; RABAL, H. Speckle time evolution characterization by the co-occurrence matrix analysis. **Optics and Laser Technology**, v. 31, n. 2, p. 163-169, 1999.

BARBOSA, N. C. **Taxa de respiração do mamão em função das diferentes condições de atmosferas de armazenamento em temperatura ambiente**. 2013. Dissertação (Mestrado em Produção Vegetal com Concentração em Tecnologia de Alimentos e Constituintes Químicos Vegetais) – Universidade Estadual do Norte Fluminense Darcy Ribeiro, Campos dos Goytacazes, 2013.

BETIN, P. S. *et al.* Avaliação do fruto da goiabeira em diferentes estádios de maturação através de métodos tradicionais e biospeckle. *In*: CONGRESSO BRASILEIRO DE ENGENHARIA AGRÍCOLA, 47., 2018, Brasília. **Anais [...]**. Brasília, DF: CONBEA, 2018.

BRAGA, R. A. *et al.* Evaluation of activity through dynamic laser speckle using the absolute value of the differences. **Optics Communications**, v. 284, n. 2, p. 646-650, 2011.

BRAGA, R. A.; RIVERA, F. P.; MOREIRA, J. **A practical guide to Biospeckle laser analysis**. Lavras: UFLA, 2016.

CAKMAK, H. Assessment of fresh fruit and vegetable quality with non-destructive methods. *In*: GALANAKIS, C. M. (ed.). **Food quality and shelf life**. [S. l.]: Elsevier, 2019.

CALBO, A. G.; MORETTI, C. L.; HENZ, G. P. *et al.* **Respiração de frutas e hortaliças**. Brasília, DF: Embrapa, 2007.

CAMELO, A.; GÓMEZ, P. Comparison of color indexes for tomato ripening. **Horticultura Brasileira**, p. 534-537, 2004.

CARDOSO, R. R. *et al.* Frequency signature of water activity by biospeckle laser. **Optics Communications**, v. 284, n. 8, p. 2131-2136, 2011.

CHITARRA, M. I. F.; CHITARRA, A. B. **Pós-colheita de frutos e hortaliças: fisiologia e manuseio**. 2. ed. Lavras: UFLA, 2005.

COLOMBIÉ, S. *et al.* Respiration climacteric in tomato fruits elucidated by constraint-based modelling. **New Phytologist**, v. 213, n. 4, p. 1726-1739, 2016.

FERREIRA, D. F. Sisvar: a computer statistical analysis system. **Ciência e Agrotecnologia**, v. 35, n. 6, p. 1039-1042, 2011.

FERREIRA, S. M. R. *et al.* Qualidade pós-colheita do tomate de mesa convencional e orgânico. **Ciência e Tecnologia de Alimentos**, v. 30, n. 4, p. 858-864, 2010.

FERREIRA, S. M. R.; QUADROS, D. A. de; FREITAS, R. J. S. de. Classificação do tomate de mesa cultivado nos sistemas convencional e orgânico. **Ciência e Tecnologia de Alimentos**, v. 25, n. 3, p. 584-590, 2005.

- INSTITUTO ADOLFO LUTZ. **Métodos físicos-químicos para análise de alimentos**. São Paulo: IAL, 2008.
- KADER, A. A. **Postharvest technology of horticultural crops**. 3. ed. California: University of California Agricultural and Natural Resources, 2002.
- LIEN, C. C.; AY, C.; TING, C. H. Non-destructive impact test for assessment of tomato maturity. **Journal of Food Engineering**, v. 91, n. 3, p. 402-407, 2009.
- MAHANTI, N. K. *et al.* Emerging non-destructive imaging techniques for fruit damage detection: image processing and analysis. **Trends in Food Science & Technology**, v. 120, p. 418-438, 2022.
- MOURA, M. L. *et al.* Fisiologia do amadurecimento na planta do tomate “Santa Clara” e do mutante “Firme”. **Horticultura Brasileira**, v. 23, n. 1, p. 81-85, 2005.
- MOURA, M. L. **Fisiologia do amadurecimento de tomates ‘Santa Clara’ e seu mutante natural ‘firme’**. 2002. 89 p. Tese (Doutorado em Fisiologia Vegetal) – Universidade Federal de Viçosa, Viçosa (MG), 2002.
- MUBAROK, S. *et al.* Data on the yield and quality of organically hybrids of tropical tomato fruits at two stages of fruit maturation. **Data in Brief**, v. 25, p. 104031, 2019.
- OULAMARA, A.; TRIBILLON, G.; DUVERNOY, J. Biological activity measurement on botanical specimen surfaces using a temporal decorrelation effect of laser speckle. **Journal of Modern Optics**, v. 36, n. 2, p. 165-179, 1989.
- PALUMBO, M. *et al.* Computer vision system based on conventional imaging for non-destructively evaluating quality attributes in fresh and packaged fruit and vegetables. **Postharvest Biology and Technology**, v. 200, p. 112332, 2023.
- PANDISELVAM, R. *et al.* Biospeckle laser technique: a novel non-destructive approach for food quality and safety detection. **Trends in Food Science & Technology**, v. 97, p. 1-13, 2020.
- RABAL, H. J.; BRAGA, R. A. **Dynamic Laser Speckle and Applications**. Florida: CRC Press, 2008.
- RABELO, G. F. *et al.* Frequency response of biospeckle laser images of bean seeds contaminated by fungi. **Biosystems Engineering**, v. 110, p. 297-301, 2011.
- RABELO, G. F.; BRAGA JÚNIOR, R. A.; FABBRO, I. M. D. *et al.* Laser speckle techniques in quality evaluation of orange fruits. **Revista Brasileira de Engenharia Agrícola e Ambiental**, v. 9, n. 4, p. 570-575, 2005.
- SCHWARZ, K. *et al.* Desempenho agrônômico e qualidade físico-química de híbridos de tomateiro em cultivo rasteiro. **Horticultura Brasileira**, v. 31, n. 3, p. 410-418, 2013.
- SHIRAHIGE, F. H. Produtividade e qualidade de híbridos de tomate (*Solanum lycopersicum* L.) dos segmentos Santa Cruz e Italiano em função do raleio de frutos, em ambiente protegido. **Horticultura Brasileira**, v. 28, n. 3, p. 292-298, 2010.
- SZYMANSKA-CHARGOT, M.; ADAMIÁK, A.; ZDUNEK, A. Pre-harvest monitoring of apple fruits development with the use of biospeckle method. **Scientia Horticulturae**, v. 145, p. 23-28, 2012.
- UNITED STATES DEPARTMENT OF AGRICULTURE. **United States standards for grades of fresh tomatoes**. [S. l.]: USDA, 1991.
- ZDUNEK, A. *et al.* The biospeckle method for the investigation of agricultural crops: a review. **Optics and Lasers in Engineering**, v. 52, n. 1, p. 276-285, jan. 2014.

